ISSN 1063-7761, Journal of Experimental and Theoretical Physics, 2017, Vol. 125, No. 2, pp. 175–188. © Pleiades Publishing, Inc., 2017.
Original Russian Text ©A.A. Zyablovskii, A.A. Pavlov, V.V. Klimov, A.A. Pukhov, A.V. Dorofeenko, A.P. Vinogradov, A.A. Lisyanskii, 2017, published in Zhurnal Eksperimental'noi i Teoreticheskoi Fiziki, 2017, Vol. 152, No. 2, pp. 211–226.

ATOMS, MOLECULES, OPTICS

Extraordinary Light Transmission Through a Metal Film Perforated by a Subwavelength Hole Array

A. A. Zyablovskii[a,b,*], A. A. Pavlov[a], V. V. Klimov[a,d,e], A. A. Pukhov[a,b,c], A. V. Dorofeenko[a,b,c], A. P. Vinogradov[a,b,c], and A. A. Lisyanskii[f,g]

[a] *Dukhov All-Russian Research Institute of Automatics, Moscow, 127055 Russia*
[b] *Moscow Institute of Physics and Technology (State University), Dolgoprudnyi, Moscow oblast, 141700 Russia*
[c] *Institute of Theoretical and Applied Electrodynamics, Russian Academy of Sciences, Moscow, 125412 Russia*
[d] *Lebedev Physical Institute, Russian Academy of Sciences, Moscow, 119991 Russia*
[e] *National Research Nuclear University "MEPhI", Moscow, 115409 Russia*
[f] *Department of Physics, Queens College of the City University of New York, New York, 11367 USA*
[g] *The Graduate Center of the City University of New York, New York, 10016 USA*
**e-mail: zyablovskiy@mail.ru*
Received January 21, 2017

Abstract—It is shown that, depending on the incident wave frequency and the system geometry, the extraordinary transmission of light through a metal film perforated by an array of subwavelength holes can be described by one of the three mechanisms: the "transparency window" in the metal, excitation of the Fabry–Perot resonance of a collective mode produced by the hybridization of evanescence modes of the holes and surface plasmons, and excitation of a plasmon on the rear boundary of the film. The excitation of a plasmon resonance on the front boundary of the metal film does not make any substantial contribution to the transmission coefficient, although introduces a contribution to the reflection coefficient.

DOI: 10.1134/S1063776117070123

1. INTRODUCTION

In 1998, Ebbesen and coworkers [1, 2] discovered experimentally extraordinary light transmission (ELT) through a metal film perforated by a period array of subwavelength holes. The transmission of light was called extraordinary because the frequency dependence of the transmission coefficient normalized to the area of holes was nonmonotonic and exceeded unity at some frequencies. This fact attracted attention to the problem of light transmission through a periodic array of holes in a metal film [3–5], because the nonmonotonic wavelength dependence of the transmission coefficient cannot be explained by considering the transmission of light through subwavelength holes in an infinitely thin ideally conducting screen [6–8]. Indeed, according to the Bethe theory [6], the transmission coefficient of light through a circular subwavelength hole in an infinitely thin ideally conducting screen normalized to the hole area is proportional to $(d/\lambda)^4$, where d is the hole diameter and λ is the light wavelength. Assuming that the transmission coefficient through each hole in the array is independent of the presence of other holes, the total transmission coefficient proves to be smaller than unity and monotonically decreases with increasing incident radiation wavelength.

In the case of a finite-thickness film, the transmission coefficient is also proportional to $(d/\lambda)^4\exp(-h\mathrm{Im}q)$, where k is the film thickness, q is the wavevector of a mode in a hole (see experimental [9, 10] and theoretical [11] works). The maximum of the transmission coefficient is observed only if the size of the hole becomes comparable with the wavelength when the mode of the hole becomes propagating [12–14]. In this case, the transmission maximum is related to the excitation of a Fabry–Perot resonance in a single hole. For a subwavelength hole, only a monotonic decrease in the transmission coefficient is observed with increasing incident radiation wavelength [15].

To explain the ELT through subwavelength holes, different mechanisms were proposed in the literature [16–20]. The nature of this effect was qualitatively discussed in [1], where ELT was explained by excitation of surface plasmons either on the front or rear boundary of a metal film. This explanation was based on experimental facts discovered in [1]. First, it was found that the transmission coefficient maxima were not observed for germanium films [1]. Because germanium has the positive permittivity in the spectral range of measurements,[1] a conclusion was made that plasmon properties of the film material are important. Second, it was shown experimentally that the wavelengths of the transmission coefficient maxima linearly depended on the array period. Third, it was found that the position of the transmission coefficient maxima depended on the angle of incidence. As the angle of incidence was changed, the intensity of maxima changed; maxima could split into two and shift. Thus, while one maximum of the transmission coefficient was observed for normal incidence, the deviation from the normal incidence caused the splitting of the maximum into two.

Ebbesen explained all these experimental facts assuming that the transmission coefficient maxima appear due to excitation of surface plasmons. The excitation condition for a surface plasmon resonance can be written in the form

$$\mathbf{k}_{\rm sp}(\omega) = \mathbf{k}_L(n,m) = \mathbf{k}_\tau + n\mathbf{G}_x + m\mathbf{G}_y, \qquad (1)$$

where $\mathbf{k}_{\rm sp}(\omega)$ is the wavevector of a surface plasmon, $\mathbf{k}_\tau$ is the tangential component of the wavevector of the incident wave, $\mathbf{G}_{x,\,y} = (2\pi/L_{x,\,y})\mathbf{e}_{x,\,y}$ is the reciprocal array vector, $\mathbf{e}_{x,\,y}$ are unit vectors along corresponding axes, n and m are integers, and $\mathbf{k}_L(n, m)$ is a vector satisfying the Laue condition. By neglecting the material dispersion, $|\mathbf{k}_{\rm sp}|$ is inversely proportional to the incident wavelength, and the wavelengths for which condition (1) is fulfilled are linearly scaled with changing the array period $L_{x,\,y}$.

For normally incident light $\mathbf{k}_\tau = 0$, the frequencies for pairs of numbers (n, m) and $(-n, -m)$ at which condition (1) is fulfilled coincide, and degeneracy is observed. For incidence at angles $\mathbf{k}_\tau \neq 0$, we have $|\mathbf{k}_L(n, m)| \neq |\mathbf{k}_L(-n, -m)|$ and this degeneracy is lifted. As a result, when the angle of incidence deviates from the normal, the transmission coefficient maxima associated with excitation of surface plasmons split into two.

Although these qualitative considerations suggest the importance of plasmon excitation, quantitative discrepancies exceed the experimental error [1]. Moreover, how plasmon excitation is related to the ELT effect remains unclear.

The possible ELT mechanism providing a quantitative agreement in some cases was proposed in [17] (see also [20, 21]), where it was shown that the transmission coefficient maxima are related to excitation of the Fabry–Perot resonance of a collective mode propagating simultaneously though all holes. The Fabry–Perot resonance excitation condition was written in the form

$$r^2 \exp(2iqh) = 1, \qquad (2)$$

where r is the coefficient of reflection of the collective mode from the inner boundary of the film, q is the complex wave number of the collective mode in the holes. An unusual feature of this resonance is that the eigenmode in subwavelength holes is not a propagating but an evanescent mode ($|\exp(2iqh)| \ll 1$). For condition (2) to be fulfilled, the reflection coefficient should be much greater than unity, which is possible in the case of the incidence of an evanescent wave. It was shown in [17] that the maximum of the reflection coefficient is observed when condition (1) for surface plasmon excitation is fulfilled. For this reason, ELT caused by excitation of Fabry–Perot resonances is observed at frequencies close to the excitation frequency of surface plasmons.

The ELT theory developed in [17] predicts the position of only a part of transmission coefficient maxima [1]. To explain other transmission coefficient maxima, it is necessary to consider additional mechanisms.

We show in this paper that, to explain all the cases of ELT through a metal film perforated by a two-dimensional array of subwavelength holes, three different mechanisms should be taken into account. First, this is the excitation of a Fabry–Perot resonance in holes [17], second, the excitation of a plasmon resonance on the rear boundary of the metal film, and, third, the presence of a "transparency window" of the metal [22]. In addition, we show that excitation of a plasmon resonance on the front boundary of the metal film makes no contribution to the transmission coefficient, although makes a contribution to the reflection coefficient. We show that the transmission coefficient maxima related to excitation of the Fabry–Perot resonance in holes decrease with increasing film thickness slower than the weakest decaying mode of an isolated hole.

2. FORMULATION OF THE PROBLEM. THE DESCRIPTION OF THE SYSTEM UNDER STUDY

To elucidate the ELT mechanisms, consider the problem of the normal incidence of a plane electromagnetic wave with frequency ω on a metal film with thickness h perforated by an array of cylindrical holes with a circular cross section with diameter d. We assume that the holes are located in the sites of a rectangular array with boundaries coinciding with axes x and y. The array periods along axes x and y are the same, $L_x = L_y = L$ (Fig. 1).

The metal film is surrounded from both sides by dielectrics with permittivities ε_1 and ε_2. The wave is incident from the side of the first dielectric. We denote

[1] The transmission coefficient was measured in [1] in the spectral range from 200 nm to 2 μm.

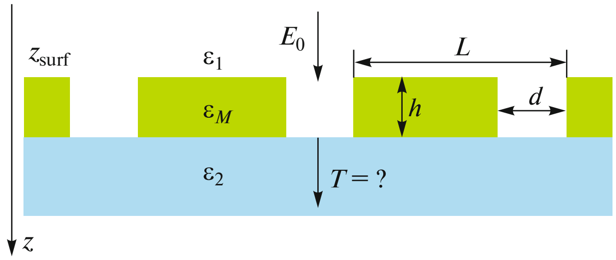

Fig. 1. Schematic view of a film perforated by holes.

the permittivity of the metal film by ε_M.[2] The z-axis is directed perpendicular to the film surface. We will make the metal film–first dielectric interface coincident with the $z = 0$ plane. In this case, the metal film–second dielectric interface will lie in the $z = h$ plane.

3. PROBLEM OF THE TRANSMISSION OF ELECTROMAGNETIC WAVES THROUGH A FINITE-THICKNESS METAL FILM WITHOUT HOLES

Note that the nonmonotonic frequency dependence of the transmission coefficient is observed even for light propagating through a continuous metal film. Consider this problem in more detail for an electromagnetic wave with frequency ω incident normally on the metal film. The transmission coefficient of the film is described by the expression [23]

$$t(\omega) = \frac{t_{1M}t_{M2}\exp(ik_{zM}h)}{1 - r_{M1}r_{M2}\exp(2ik_{zM}h)}. \quad (3)$$

Here, r_{M1} and r_{M2} are reflection coefficients of metal–first dielectric and metal–second dielectric interfaces; t_{1M} and t_{M2} are transmission coefficients for metal–first dielectric and second dielectric–metal interfaces; $k_{zM} = \sqrt{k_0^2\varepsilon_M}$ is the normal component of the wavevector in metal; $k_{z1} = \sqrt{k_0^2\varepsilon_1}$ and $k_{z2} = \sqrt{k_0^2\varepsilon_2}$ are normal components of the wavevector in the first and second dielectrics, $k_0 = \omega/c$.

Transmission coefficient (3) has a maximum at the incident light wavelength $\lambda \approx 500$ nm (Fig. 2a). The maximum appears because at $\lambda \approx 500$ nm, gold has a "transparency window" when the imaginary part $\mathrm{Im}k_{zM}$ of the normal component of the wave number has a minimum (Fig. 3a) resulting in a maximum of the exponential in the numerator in (3).

The imaginary part $\mathrm{Im}k_{zM} = k_0\mathrm{Im}\sqrt{\varepsilon_M}$ of the normal component of the wave number is independent of the system geometry and is determined exclusively by the permittivity of gold (Fig. 3b). Drastic changes in the real and imaginary parts of the gold permittivity at the wavelength $\lambda \approx 500$ nm is explained by the fact that for $\lambda < 500$ nm the interband transitions in gold begin to play an important role.

[2] We assume in calculations that the film is made of gold with the permittivity taken from [22].

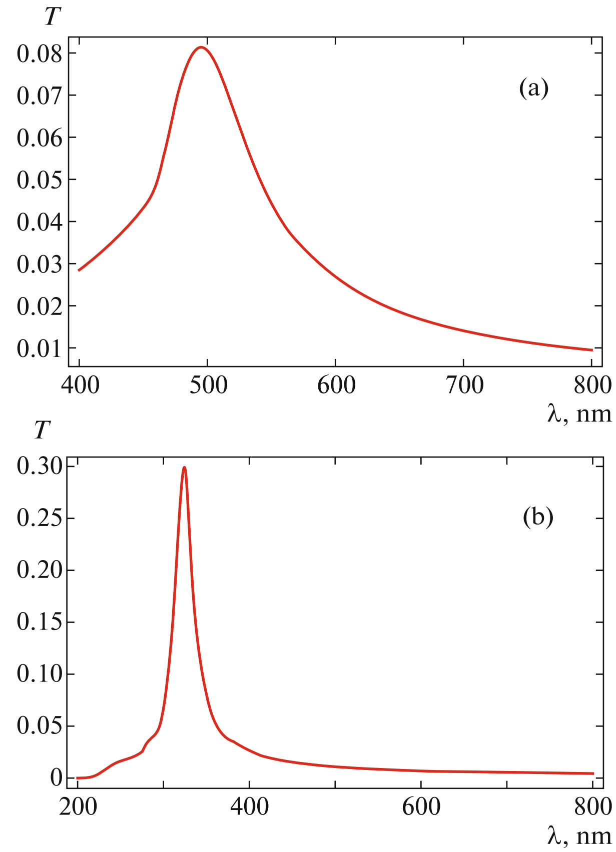

Fig. 2. Wavelength dependences of the transmission coefficient of gold (a) and silver (b) films without holes for normally incident light.

In the case of the normal incidence of light on a silver film, the transmission coefficient maximum is observed at the wavelength $\lambda \approx 300$ nm (Fig. 2b). It appears by the same reasons (Figs. 3c, 3d).

To consider the ELT problem in a metal film perforated by a hole array, it is necessary to determine the eigenmodes of this film. Consider an infinite space filled with gold and perforated by a periodic array of infinitely long circular cylinders. Then, electric and magnetic fields are periodic with the array period

$$\mathbf{E}(x, y) = \mathbf{E}(x + Ln, y + Lm),$$

$$\mathbf{H}(x, y) = \mathbf{H}(x + Ln, y + Lm),$$

where n and m are integers and L is the array period.

4. EIGENMODES OF A CIRCULAR CYLINDRICAL HOLE IN A CONTINUOUS METAL

We begin with expressions for the fields of eigenmodes and eigenwavevectors of a single hole [24, 25], which we will use below. In the case of a single hole,

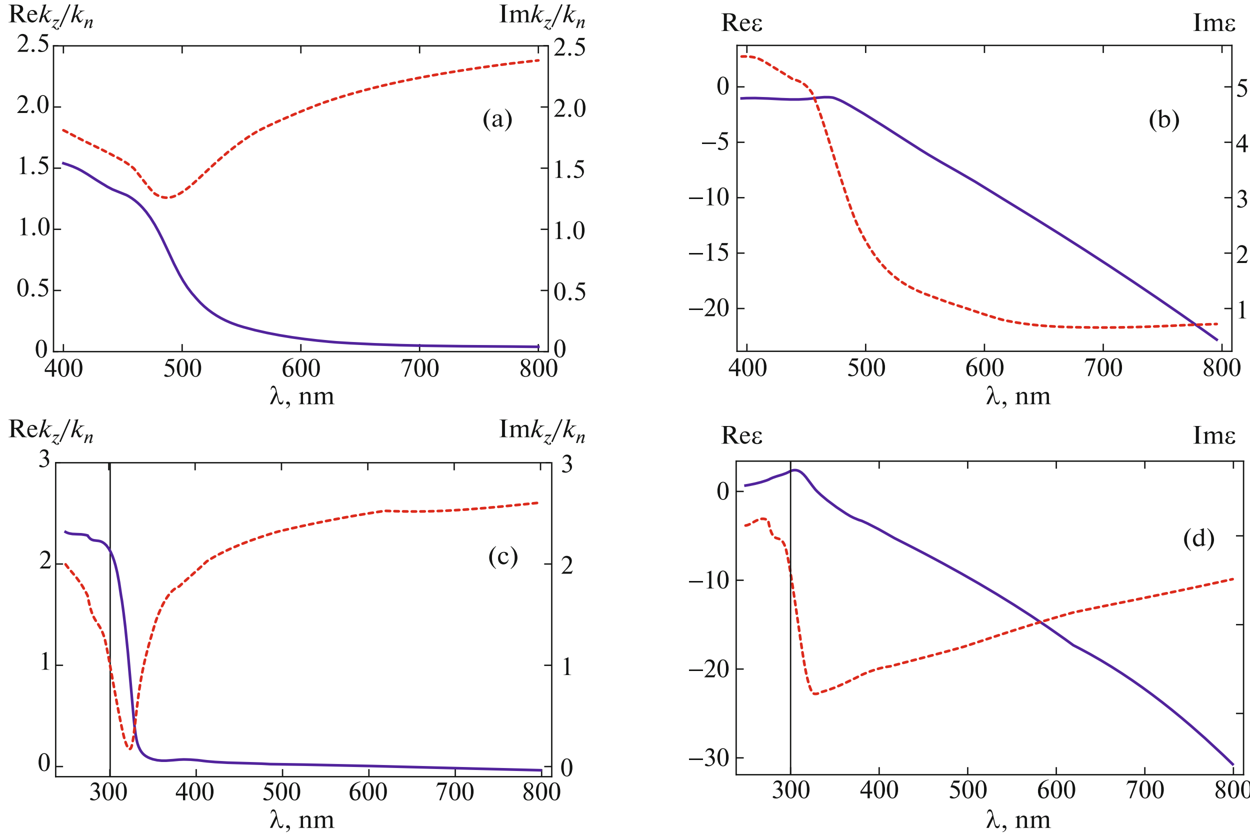

Fig. 3. Real (solid curves) and imaginary (dashed curves) parts of the normal component of the wavevector in gold (a) and silver (c) as functions of the wavelength. Real (solid curves) and imaginary (dashed curves) parts of the permittivity of gold (b) and silver (d) as functions of the wavelength. $k_n = 2\pi/400\ \text{nm}^{-1}$.

the problem is cylindrically symmetric and therefore electric and magnetic fields can be conveniently written in cylindrical coordinates $\mathbf{E}(r, \varphi, z)$ and $\mathbf{H}(r, \varphi, z)$, where r is the distance from the hole center and φ is the rotation angle in the xy plane.

The dispersion equation describing modes of a cylinder with diameter d with the permittivity ε_1 and permeability μ_1 located in a medium with the permittivity ε_M and permeability μ_M [24, 25] has the form

$$\left(\frac{\mu_M}{k_M d}\frac{J_n'(k_M d)}{J_n(k_M d)} - \frac{\mu_1}{k_1 d}\frac{H_n'(k_1 d)}{H_n(k_1 d)}\right) \times \left(\frac{\varepsilon_M}{k_M d}\frac{J_n'(k_M d)}{J_n(k_M d)} - \frac{\varepsilon_1}{k_1 d}\frac{H_n'(k_1 d)}{H_n(k_1 d)}\right) = n^2\frac{q_z^2}{k_0^2}\left(\frac{1}{k_M^2 d^2} - \frac{1}{k_1^2 d^2}\right)^2. \quad (4)$$

Here, n is a natural number or zero; J_n and H_n are Bessel and Hankel functions of order n, respectively; J_n' and H_n' are their derivatives; d is the diameter of the hole mode; $k_M = \sqrt{\varepsilon_M\mu_M k_0^2 - q_z^2}$; $k_1 = \sqrt{\varepsilon_1\mu_1 k_0^2 - q_z^2}$; and q_z is the wavevector of the hole mode.

For the nth eigenmode of the hole, all the components of electric and magnetic fields are proportional to the factor

$$\exp(-i\omega t + iq_z z + in\theta). \quad (5)$$

For any value of n, the infinite countable set of solutions of Eq. (4) exists, which can be numerated with an additional subscript m [24, 25].

The eigenmodes of the hole are separated into TM and TE modes. For $n = 0$, such a separation is obvious. The solutions of the equation

$$\frac{\mu_M}{k_M d}\frac{J_0'(k_M d)}{J_0(k_M d)} - \frac{\mu_1}{k_1 d}\frac{H_0'(k_1 d)}{H_0(k_1 d)} = 0 \quad (6)$$

are TE modes, while solutions of the equation

$$\frac{\varepsilon_M}{k_M d}\frac{J_0'(k_M d)}{J_0(k_M d)} - \frac{\varepsilon_1}{k_1 d}\frac{H_0'(k_1 d)}{H_0(k_1 d)} = 0 \quad (7)$$

are TM modes. For all other values of n, the rigorous separation into TE and TM modes is impossible.

Table 1. Wave numbers of TE eigenmodes of a single hole

$n = 0$	$n = 1$	$n = 2$
$q_{nz} \approx (0.05 + 3.3i)k_n$	$q_{nz} \approx (0.023 + 1.4i)k_n$	$q_{nz} \approx (0.0337 + 2.69i)k_n$

Consider the case when ε_1, $\mu_1 = 1$, $\mu_M = 1$, and ε_M is the gold permittivity. The wave numbers q_z of the mode of a hole with diameter $d = 150$ nm for the wavelength $\lambda = 645$ nm and different n are presented in Table 1.

Electric and magnetic fields in modes with $n = 0$ are independent of the angle and, therefore, such modes are not excited by a plane electromagnetic wave normally incident on the hole [26].

The TE mode with $n = 1$ (TE_{11}) has the smallest imaginary part $\mathrm{Im}q_z$ part of the wavevector. In addition, as shown in [26], a plane wave normally incident on a cylindrical waveguide with walls made of an ideal conductor excites only one TE_{11} mode. Therefore, in the first approximation we can consider only the TE_{11} mode.[3] The wavelength dependence of $\mathrm{Im}q_z$ for such a mode is shown in Fig. 4.

One can see from Fig. 4b that the minimum of $\mathrm{Im}q_z$ is observed at $\lambda \approx 500$ nm. As in the case of a film without holes, this minimum is related to the "transparency window" of gold (Figs. 3b, 3d). As the wavelength decreases from 800 to 500 nm, the modulus of the real part of gold permittivity decreases (Fig. 3b), achieving a maximum near 500 nm. The decrease in the modulus $|\mathrm{Re}\varepsilon_M|$ of the real part of permittivity leads to the increase in the penetration depth of the field in metal. As a result, the effective size of the hole increases leading to the decrease in $\mathrm{Im}q_z$. At wavelengths above 500 nm, the real part $\mathrm{Re}\varepsilon_M$ of the gold permittivity almost does not change, while the imaginary part $\mathrm{Im}\varepsilon_M$ drastically increases (Fig. 3b). The increase in the imaginary part of permittivity results in the increase in losses, thereby increasing $\mathrm{Im}q_z$.

Thus, the value of $\mathrm{Im}q_z$ is determined by two factors. The decrease in the modulus of the real part of permittivity results in the decrease in $\mathrm{Im}k_z$, while the increase in the imaginary part of permittivity leads to the increase in $\mathrm{Im}k_z$. For gold at $\lambda > 500$ nm, the first factor dominates and for $\lambda < 500$ nm, the second factor dominates. As a result, at $\lambda \approx 500$ nm, when the influence of these two factors becomes the same, the minimum of $\mathrm{Im}q_z$ appears.

Note that both the minimum of the imaginary part $\mathrm{Im}k_z$ of the normal component of the wavevector in gold and the minimum of the imaginary part $\mathrm{Im}q_z$ of the wavevector in the hole are observed at wavelengths close to the "transparency window" of gold. However, their positions do not exactly coincide (Fig. 5). This is explained by the fact that $\mathrm{Im}k_z$ depends only on the metal permittivity, while $\mathrm{Im}q_z$ is determined from expression (4) and depends both on the metal permittivity and the permittivity of a material filling the hole, the hole diameter, the mode number, etc.

Light waves incident on a metal film perforated by a periodic array of holes can propagate both through holes and directly through the metal. Therefore, when the intensities of waves propagated through holes and metal are close, the transmission coefficient has two (or more) maxima at wavelength close to the "transparency window" of gold.

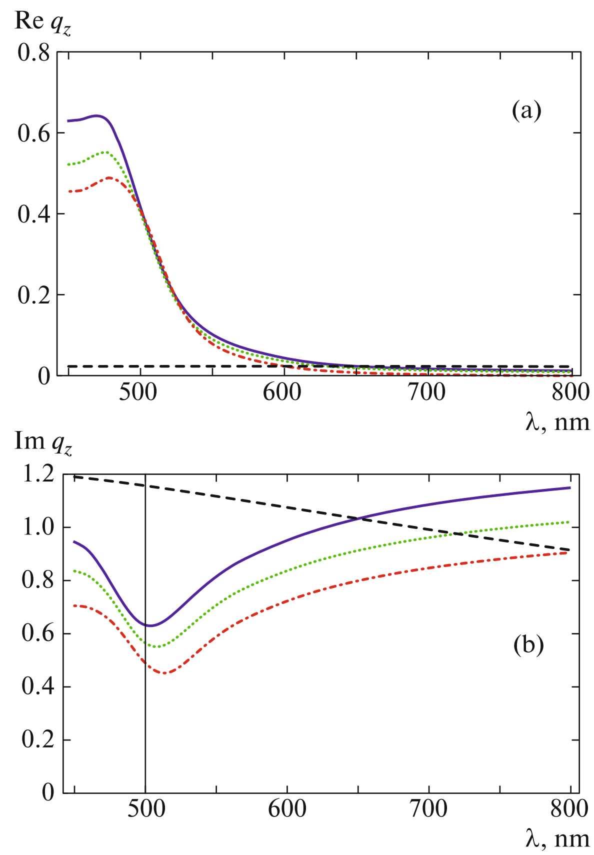

Fig. 4. Wavelength dependences of $\mathrm{Re}q_z$ (a) and $\mathrm{Im}q_z$ (b) for the TE_{11} mode (in units $k_n = 2\pi/645\ \mathrm{nm}^{-1}$). The hole diameter is 100 nm (solid curves), 125 nm (dotted curves), 150 nm (dash-and-dot curves). The hole diameter is 100 nm (dashed curves) and the permittivity of the film material is frequency-independent and equal to the gold permittivity at $\lambda = 645$ nm.

[3] Modes with $n \neq 1$ are excited because the modes of a periodic system do not coincide with the modes of a single hole. However, when the distance between holes greatly exceeds the skin layer thickness, this difference can be neglected.

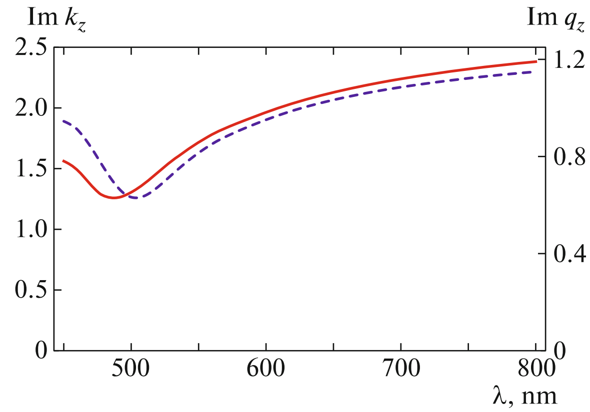

Fig. 5. Wavelength dependences of Imk_z (solid curve) and Imq_z (dashed curve) in a hole with diameter 100 nm, $k_n = 2\pi/645\ \text{nm}^{-1}$.

Note that the field-mode distribution for a single hole in a metal film differs from the field distribution in one of the holes for the mode of a hole array shown in Fig. 1. However, we will consider below only a practically important case when the hole diameter d = 100–150 nm and L = 400–600 nm. In this case, the filed tunneling from one hole to the adjacent hole is $e^8 \approx 3000$ times weaker than the field on the hole itself.[4] Therefore, we can assume with good accuracy that modes of a single hole coincide with modes in a periodic array of holes.

5. LIGHT TRANSMISSION THROUGH A FINITE-THICKNESS METAL FILM PERFORATED BY A PERIODIC HOLE ARRAY

We showed in Section 3 that the transmission coefficient of a metal film without holes for a TM-polarized wave has sharp maxima related to "transparency windows" of metals. Consider now the problem of transmission of an electromagnetic wave through a metal film perforated by a hole array.

5.1. Where Transmission Coefficient Maxima Come from

For a plane electromagnetic wave normally incident on a metal film perforated by a periodic array of holes, the waves reflected from and transmitted through the film can be expanded into a Fourier series in plane waves with wavevectors

$$\mathbf{k}_{nm} = \frac{2\pi}{L} n \mathbf{e}_x + \frac{2\pi}{L} m \mathbf{e}_y. \quad (8)$$

Here, $\mathbf{e}_z$ and $\mathbf{e}_y$ are unit vectors along the x- and y-axes, n and m are integers. To find the amplitude of such harmonics, we should determine currents on a specified boundary.[5]

A plane electromagnetic wave incident on a metal film perforated by a periodic hole array excites the eigenmodes of the film. Earlier we calculated the eigenmodes of a single hole in a continuous metal. When the distance between adjacent holes greatly exceeds the skin-layer thickness, the field from one hole does not virtually penetrate into adjacent holes and the eigenmodes of the periodic hole array can be treated as the combination of eigenmodes of separate holes. In other words, the field distribution $\mathbf{E}_{AH}(x, y, z)$ in the eigenmodes of the periodic hole array can be represented as the sum

$$\mathbf{E}_{AH}(x,y,z) \approx \sum_{n=-\infty}^{\infty} \sum_{m=-\infty}^{\infty} \mathbf{E}_{SH}(x + Ln, y + Lm, z), \quad (9)$$

where $\mathbf{E}_{SH}(x, y, z)$ is the field distribution in the eigenmode of a single hole. We took into account in (9) that the plane wave is incident normally and, as a result, the phase difference between fields in different holes is zero.

Except modes obtained by combining the eigenmodes of separate holes (9), the eigenmodes of the periodic hole array also include modes analogous to plane waves in a metal film without holes.

To solve the ELT problem, it is necessary to find the amplitudes of all these eigenmodes excited by the normally incident plane wave. To do this, it is necessary to use the continuity conditions for tangential components of electric and magnetic fields.

If the amplitudes of eigenmodes on the front boundary of a metal film are $t_N^{(1)}$, then the eigenmode amplitudes on the rear boundary of the metal film will be $t_N^{(1)}\exp(iq_N h)$, where q_N is the wavevector of the Nth mode of a hole. Hereafter, the subscript "N" denotes simultaneously toe subscripts (n, m) numerating the eigenmodes of the hole (see Section 4). It was shown in the previous section that the eigenmodes of a hole have different decay increments. When one of the modes decays much slower than all other modes (the TE_{11} mode in our case), we can assume that the amplitude of this mode is $t_1^{(1)}\exp(iq_1 h)$ and the amplitudes of all other modes can be neglected. This approximation cannot be applied if the coefficient $t_K^{(1)}$ for some Kth mode will greatly exceed the coefficient $t_1^{(1)}$. We will show below that this approximation is valid for our system. Here, we recall that in the case of a single hole,

[4] The minimal distance between hole boundaries in this case is 250 nm, while the skin layer thickness in a gold film is about 30 nm.

[5] In practice, it is sufficient to know only the amplitudes of plane wave which are not evanescent.

a normally incident plane electromagnetic wave excites only the TE_{11} mode (see the previous section). In the case of a hole array, because of the break of the cylindrical symmetry, only modes with $n \neq 1$ can be excited, however, their amplitudes will be small for a large enough distance between holes. This justifies our approximation.

A mode with the amplitude $t_N^{(1)}\exp(iq_N h)$ incident on the rear boundary of a metal film is partially reflected the coefficient $r_N^{(2)}$ and partially penetrates into the dielectric. The reflected wave will be again a sum of all the eigenmodes of the system with amplitudes $t_N^{(1)} r_{NM}^{(2)} \exp(iq_N h)$, where M is the number of the reflected mode. The amplitudes of eigenmodes will decrease during propagation from the rear boundary of the metal plane to its front boundary and will be equal to $t_N^{(1)} r_{NM}^{(2)} \exp(i(q_N + q_M)h)$ on the front boundary. Assuming that the decay decrement of the TE_{11} mode is the smallest, we can assume again that the amplitudes of all other modes of the front boundary are zero. The TE_{11} mode is partially reflected back from the front boundary with the coefficient $r_N^{(1)}$ and partially penetrated into the dielectric under over the film. By repeating these considerations for the reflected wave, we finally obtain the expression for the amplitude t_{nm} of the wave with the wavevector $\mathbf{k}_{nm}$ escaping from the film on its rear boundary

$$t_{nm} = \frac{t_N^{(1)} t_{Nnm}^{(2)} \exp(iq_N h)}{1 - r_N^{(1)} r_N^{(2)} \exp(2iq_N h)}. \tag{10}$$

Here, $t_N^{(1)}$ is the amplitude of the Nth mode on the front boundary of the metal film excited by the incident plane wave with the unit amplitude, $t_{Nnm}^{(2)}$ is the amplitude of a plane wave with the wavevector $\mathbf{k}_{nm}$ on the rear boundary of the metal film excited by the incident N mode with the unit amplitude, and $r_N^{(1)}$ and $r_N^{(2)}$ are reflection coefficients of the N mode from the front and rear boundaries of the metal film.

It is important to emphasize that we calculated reflection coefficients $r_N^{(1)}$ and $r_N^{(2)}$ and transmission coefficients $t_N^{(1)}$ and $t_N^{(2)}$ taking into account all the eigenmodes of the metal film perforated by the hole array. However, we also assume that the amplitudes of all eigenmodes except the TE_{11} mode decrease to zero during propagation from one boundary of the metal film to the other.

The maxima of transmission coefficient (10) can be observed in the following cases:

(i) If q_N has a local minimum at a certain frequency. In real systems, the minima of q_N appear due to the presence of "the transparency window" in metals (see the previous section);

(ii) if coefficients $t_N^{(1)}$ or $t_N^{(2)}$ have maxima in frequency;

(iii) if the dominator of expression (10) vanishes,

$$r_N^{(1)} r_N^{(2)} \exp(2iq_N h) = 1. \tag{11}$$

This condition can be represented in the form of two conditions for the amplitude and phase

$$\exp(-2h\,\mathrm{Im}\,q_N) = \frac{1}{|r_N^{(1)}||r_N^{(2)}|}, \tag{12}$$

$$\arg(r_N^{(1)} r_N^{(2)}) - 2h\,\mathrm{Re}\,q_N = 2\pi j, \tag{13}$$

where j is an integer. One can see from the table that for the film thickness $h = 100$ nm, the phase incursion after the propagation of the $n = 1$ mode through the hole is $h\mathrm{Re}q_N \approx 0.023$ rad. Thus, for the $n = 1$ mode, condition (13) is fulfilled when $\arg(r_N^{(1)} r_N^{(2)}) \approx 2\pi j$.[6] Such a mode is the "zero" Fabry–Perot resonance, when the zero number of wavelengths fits in the hole length.

To determine frequencies at which the transmission coefficient maxima related to resonances in holes are observed, it is necessary to calculate the coefficients of reflection of the hole mode from the hole–dielectric interface.

5.2. Calculation of the Coefficient $t_N^{(1)}$

Consider a plane wave with the unit amplitude incident on an infinite-thickness metal film perforated by a periodic hole array. To find the coefficient $t_N^{(1)}$, we will write the continuity conditions for tangential components of electric and magnetic fields separately for each Fourier harmonic. It follows from continuity conditions for the tangential component of the magnetic field that

$$H_0(x, y) + H^r(x, y) = H^t(x, y), \tag{14}$$

where $H_0(x, y)$ and $H^r(x, y)$ are tangential components of the incident and reflected magnetic fields and $H^t(x, y)$ is the tangential component of the magnetic field penetrated into the film. The latter term can be expanded in the eigenmodes of the system as

$$H^t(x, y) = \sum_N t_N^{(1)} H^{(N)}(x, y). \tag{15}$$

Here, $H^{(N)}(x, y)$ is the field distribution in the Nth eigenmode of the system and $t_N^{(1)}$ are expansion coefficients.

[6] Similarly, for modes with $n = 0$ and $n = 2$.

By expanding $H^{(N)}(x, y)$, $H_0(x, y)$ and $H^r(x, y)$ in Fourier series, we pass from Eq. (14) to the equation

$$\sum_{n,m}\delta_{0n}\delta_{0m}\exp\left(i\frac{2\pi x}{L}n+i\frac{2\pi y}{L}m\right)$$
$$+\sum_{n,m}h^r_{nm}\exp\left(i\frac{2\pi x}{L}n+i\frac{2\pi y}{L}m\right) \quad (16)$$
$$=\sum_N t^{(1)}_N\sum_{n,m}h^{(N)}_{nm}\exp\left(i\frac{2\pi x}{L}n+i\frac{2\pi y}{L}m\right).$$

Here, h^r_{nm} and $h^{(N)}_{nm}$ are Fourier expansion coefficients for fields $H^r(x, y)$ and $H^{(N)}(x, y)$. By changing the summation order in the right-hand side of (16) and taking into account that the equality should be fulfilled for any values of x and y, we obtain the continuity condition separately for each Fourier harmonic,

$$\delta_{0n}\delta_{0m}+h^r_{nm}=\sum_N t^{(1)}_N h^{(N)}_{nm}. \quad (17)$$

Similarly, we can obtain the continuity equation for each Fourier harmonic of the tangential component of the electric field,

$$\delta_{0n}\delta_{0m}+e^r_{nm}=\sum_N t^{(1)}_N e^{(N)}_{nm}. \quad (18)$$

Using Eqs. (17) and (18), we can find the coefficients of expansion in the eigenmodes $t^{(1)}_N$ of the system for the field propagated through the metal field boundary. To do this, it is necessary to express the Fourier harmonics e^r_{nm} and $e^{(N)}_{nm}$ of the electric field in terms of the Fourier harmonics of the magnetic field, which allows one to obtain a closed system of equations for coefficients $t^{(1)}_N$.

Each Fourier harmonic $\mathbf{h}^{(N)}_{nm}$ of the magnetic field is perpendicular to the wavevector $\mathbf{k}^{(N)}_{nm}$ and to the corresponding Fourier harmonic $\mathbf{d}^{(N)}_{nm}$, while the electric induction is perpendicular to the wavevector [27],

$$\mathbf{k}^{(N)}_{n,m}\times\mathbf{h}^{(N)}_{nm}=-\frac{\omega}{c}\mathbf{d}^{(N)}_{nm}, \quad (19)$$

where

$$\mathbf{k}^{(N)}_{n,m}=\left(\frac{2\pi}{L}n,\frac{2\pi}{L}m,q_N\right).$$

It follows from Eq. (19) that tangential components of the electric induction and magnetic field are related by the expression

$$d^{(N)}_{nm}=-\frac{q_N}{\omega/c}h^{(N)}_{nm}. \quad (20)$$

To express the continuity equations for the electric field in terms of magnetic-field components, we will use the equation relating the electric induction with the electric field:

$$\mathbf{d}^{(N)}_{nm}=\sum_{j=-\infty}^{\infty}\sum_{l=-\infty}^{\infty}\varepsilon_{ij}\mathbf{e}^{(N)}_{n-j,m-l}, \quad (21)$$

where ε_{ij} are Fourier expansion coefficients of the permittivity. From (21), we express the tangential component of the electric field in terms of the tangential component of the electric induction:

$$e^{(N)}_{nm}=\hat{\varepsilon}^{-1}d^{(N)}_{nm}, \quad (22)$$

where $\hat{\varepsilon}^{-1}$ is a tensor inverse to the permittivity tensor

$$\hat{\varepsilon}\mathbf{e}^{(N)}_{n,m}=\sum_{j=-\infty}^{\infty}\sum_{l=-\infty}^{\infty}\varepsilon_{ij}\mathbf{e}^{(N)}_{n-j,m-l}.$$

By using Eqs. (20) and (22), we rewrite the continuity equation of the tangential component of the electric field (18) in terms of tangential components of the magnetic field,

$$\frac{k_z}{\varepsilon_1}(\delta_{0n}\delta_{0m}-h^r_{nm})=\hat{\varepsilon}^{-1}\sum_N q_N h^{(N)}_{nm}t^{(1)}_N. \quad (23)$$

Here, $h^{(N)}_{nm}$ are Fourier expansion coefficients for the Nth mode, h^r_{nm} is tangential component of the magnetic field in the reflected wave with the wavevector (8), $k_z=\sqrt{\varepsilon_{1,2}k_0^2-k^2_{nm}}$ is the normal component of the wavevector in a dielectric, and q_N is the wavevector of the Nth mode.

Equations (17) and (23) form a closed system of equations for coefficients $t^{(1)}_N$. Below, we will calculate coefficients $t^{(1)}_N$ taking into account a finite number of Fourier harmonics and a finite number of eigenmodes of the system. To define the system of equations for coefficients $t^{(1)}_N$, we will take into account equal numbers of Fourier harmonics and eigenmodes of the system.

Note that Eqs. (16)–(23) neglect the excitation of waves with polarization different from that of the incident wave. In the case of a plane wave normally incident on a single hole, waves with such polarization are not excited because of the cylindrical symmetry of the problem.

Upon the normal incidence of a plane wave on a film perforated by a periodic array circular holes, polarization is preserved if the polarization of the incident wave is directed along one of the vectors of this array. In the general case, polarizations of the reflected and transmitted waves can differ from that of the incident wave. Polarization changes because the eigenmodes of the system differ from the modes of a single hole and do not have the cylindrical symmetry.

In this work, we consider the case when the distance between holes greatly exceeds the skin-layer thickness and fields in different holes weakly affect each other. As a result, polarizations of the reflected and transmitted waves weakly differ (or do not differ at all) from polarization of the incident wave.

5.3. Calculation of Coefficients $t_N^{(2)}$, $r_N^{(1)}$, and $r_N^{(2)}$

The reflected field of the *N*th mode incident on the hole in metal–dielectric interface is a sum of all the modes of the system with coefficients r_{NM}. To find coefficients r_{NM} (we are interested first of all in the coefficient $r_N = r_{NN}$), we write the continuity condition for each Fourier harmonic on the boundary of tangential components of electric and magnetic fields for the TM mode,

$$h_{nm}^{(N)} + \sum_M r_{NM} h_{nm}^{(M)} = h_{nm}^t, \tag{24}$$

$$\hat{\varepsilon}^{-1}\left(q_N h_{nm}^{(N)} - \sum_M q_M r_{NM} h_{nm}^{(M)}\right) = \frac{k_z}{\varepsilon_{1,2}} h_{nm}^t, \tag{25}$$

where $k_z = \sqrt{\varepsilon_{1,2}k_0^2 - k_{nm}^2}$ is the normal component of the wavevector in the dielectric, q_N is the wavevector of the *N*th mode, $h_{nm}^{(M)}$ are Fourier expansion coefficients for the *M*th mode, and h_{nm}^t is the wave amplitude in the dielectric with the tangential component of the wavevector (8).

By solving the system of equations (24), (25), we obtain the values of coefficients r_{NM} from which the required coefficients $r_N^{(1)}$ (or $r_N^{(2)}$) are equal to r_{NN}. The coefficient $t_N^{(2)}$ is also found from system (24), (25) and is equal to h_{nm}^t.

6. DETERMINATION OF THE WAVELENGTHS OF TRANSMISSION COEFFICIENT MAXIMA IN THE CASE OF A SMALL-DIAMETER HOLE

6.1. Limit of Infinitesimal-Diameter Holes

Knowing the wave numbers q_N of the eigenmodes of the system and coefficients $t_N^{(1)}$, $t_N^{(2)}$, $r_N^{(1)}$, and $r_N^{(2)}$, we can find the wave amplitude t_{nm} with the wavevector $\mathbf{k}_{nm}$ on the rear boundary of the metal film (10). However, systems of equations (17), (23), and (24), (25) are infinite systems of linear equations and do not admit an analytic solution.

To obtain analytic expressions for coefficients $t_N^{(1)}$, $t_N^{(2)}$, $r_N^{(1)}$, and $r_N^{(2)}$, we consider the limit of an infinitesimal-diameter hole ($k_0 d \to 0$). In this case, the wave numbers of all modes become identical[7] and the matrix $\hat{\varepsilon}^{-1}$ becomes diagonal with diagonal elements equal to ε_M^{-1}, which allows us to pass from systems of equations (17), (23) and (24), (25) to two systems of equations

$$\delta_{n0}\delta_{m0} + h_{nm}^r = h_{nm}^{tr}, \tag{26}$$

$$\frac{k_z^{nm}}{\varepsilon_{1,2}}(\delta_{n0}\delta_{m0} - h_{nm}^r) = \frac{q}{\varepsilon_M} h_{nm}^{tr} \tag{27}$$

and

$$h_{nm}^{(N)} + h_{nm}^{\text{ref}} = h_{nm}^t, \tag{28}$$

$$\frac{q}{\varepsilon_M}(h_{nm}^{(N)} - h_{nm}^{\text{ref}}) = \frac{k_z^{nm}}{\varepsilon_{1,2}} h_{nm}^t. \tag{29}$$

Here, q is the wave number of hole modes in the case when the hole diameter tends to zero, h_{nm}^{tr} is the magnetic field amplitude in the reflected wave for the *N* mode,

$$h_{nm}^{tr} = \sum_M t_M^{(1)} h_{nm}^{(N)} = S_{nmM} t_M^{(1)}, \tag{30}$$

and h_{nm}^{ref} is the magnetic field amplitude in the reflected wave,

$$h_{nm}^{\text{ref}} = \sum_M r_{NM} h_{nm}^{(M)} = S_{nmM} r_{NM}, \tag{31}$$

where S_{nmM} is a matrix with the *nmM*th element equal to $h_{nm}^{(M)}$. It follows from Eqs. (30) and (31) that

$$t_M^{(1)} = S_{nmM}^{-1} h_{nm}^{tr}, \tag{32}$$

$$r_{NM} = S_{nmM}^{-1} h_{nm}^{\text{ref}}. \tag{33}$$

It follows from the system of equations (26), (27) that

$$h_{nm}^{tr} = \frac{2\varepsilon_M k_z^{nm}}{\varepsilon_M k_z^{nm} + \varepsilon_{1,2} q}\delta_{n0}\delta_{m0}. \tag{34}$$

In turn, it follows from the system of equations (28), (29) that

$$h_{nm}^{\text{ref}} = \frac{\varepsilon_{1,2} q - \varepsilon_M k_z^{nm}}{\varepsilon_{1,2} q + \varepsilon_M k_z^{nm}} h_{nm}^{(N)}. \tag{35}$$

[7] Indeed, in the limit $k_0 d \to 0$ for $n \neq 0$, we obtain $J_n'(k_0 d)/J_n(k_0 d) \to n/k_0 d$ and $H_n'(k_0 d)/H_n(k_0 d) \to -n/k_0 d$. As a result, dispersion equation (4) no longer depends on the mode number *n*.

Here, ε_M and $\varepsilon_{1,2}$ are permittivities of the metal and dielectric, the subscript "1" corresponds to reflection from the front boundary of the film and the subscript "2" to reflection from the rear boundary.

As a result, we obtain

$$t_M^{(1)} = \frac{2\varepsilon_M k_z^{nm}}{\varepsilon_M k_z^{nm} + \varepsilon_{1,2} q} S_{nmM}^{-1} \delta_{n0} \delta_{m0}, \tag{36}$$

$$r_{NM} = \frac{\varepsilon_{1,2} q - \varepsilon_M k_z^{nm}}{\varepsilon_{1,2} q + \varepsilon_M k_z^{nm}} S_{nmM}^{-1} h_{nm}^{(N)}. \tag{37}$$

Coefficients $t_M^{(1)}$ and r_{NM} have maxima when the resonance condition

$$\varepsilon_{1,2} q + \varepsilon_M k_z^{nm} = 0 \tag{38}$$

is fulfilled.

However, the coefficient $t_M^{(1)}$ is nonzero only for $n = m = 0$, when $k_z^{00} = \omega/c$ and therefore resonance condition (38) is never fulfilled for $t_M^{(1)}$. Coefficients r_{NM} are nonzero for arbitrary n and m and resonance condition (38) can be fulfilled.

For all modes with $n \neq 0$, the wavevector q tends to $k_0\sqrt{\varepsilon_M}$ for $k_0 d \neq 0$. Therefore, condition (38) is fulfilled when the modulus of the tangential component of the wavevector $\mathbf{k}_{nm}$ (38) is

$$|\mathbf{k}_{nm}| = k_{\text{res}} = \frac{\omega}{c} \text{Re}\left[\sqrt{\frac{\varepsilon_{1,2}(\varepsilon_M - \varepsilon_{1,2})}{\varepsilon_M}}\right]. \tag{39}$$

Note that for $|\varepsilon_M| \gg \varepsilon_{1,2}$, the relation

$$k_{\text{res}} \approx k_{sp} = \frac{\omega}{c} \text{Re}\left[\sqrt{\frac{\varepsilon_{1,2}\varepsilon_M}{\varepsilon_M + \varepsilon_{1,2}}}\right], \tag{40}$$

takes place, where k_{sp} is the real part of the wave number of a surface plasmon on the metal–dielectric boundary. In other words, the maximum of the reflection coefficient r_{NM} is observed when the tangential component of the wavevector of the incident wave is equal to the wavevector of a surface plasmon.

Thus, reflection coefficients $r_N^{(1)}$ and $r_N^{(2)}$ (i.e., r_{NN}) have maxima when condition (39) is fulfilled. In the case of subwavelength holes, eigenmodes are evanescent and therefore $\exp(-2h\,\text{Im}\,q_N) \to 0$ with increasing the film thickness. In this case, Fabry–Perot resonances in holes can be observed only when $|r_N^{(1,2)}| \gg 1$ (see the amplitude Fabry–Perot resonance condition (12)). Therefore, the position of the transmission coefficient maxima in thick films is determined by condition (39), which for $|\varepsilon_M| \gg \varepsilon_{1,2}$ is close to the excitation condition of a surface plasmon on the metal–dielectric interface.

Transmission coefficient maxima (10) can be related not only to Fabry–Perot resonances in a hole, but also to the maxima of $t_N^{(2)}$ (the excitation coefficient of a plane wave with the tangential component of the wavevector $\mathbf{k}_{nm}$ by the Nth mode on the rear boundary of the metal film). When the hole diameter $k_0 d \to 0$, the coefficient $t_N^{(2)}$ is determined from the system of equations (28), (29),

$$t_N^{(2)} = \frac{2\varepsilon_M k_z}{\varepsilon_{1,2} q + \varepsilon_M k_z}. \tag{41}$$

Thus, the positions of $t_N^{(2)}$ maxima coincides with that of k_{NM} maxima.

The transmission coefficient t_{nm} of a metal film perforated by a hole array is proportional to $t_N^{(2)}$ (see Eq. (10)), therefore, independent of the film thickness, the position of transmission coefficient maxima is determined by condition (38). For $|\varepsilon_M| \gg \varepsilon_{1,2}$, this is the excitation condition for a surface plasmon on the metal–dielectric boundary.

Note, however, that condition (38) is fulfilled only for waves with the tangential component of the wavevector $k_{\text{res}} > (\omega/c)\varepsilon_{1,2}$. Therefore, such waves exponentially decrease with increasing distance from the metal film surface and do not contribute to the transmitted radiation intensity.

As a result, in the limit of an infinitesimal hole diameter $k_0 kd \to 0$, the intensity maxima of transmitted radiation can be related only to Fabry–Perot resonances in holes in the metal film. We will show below that, when a finite diameter of the hole is taken into account, the intensity maxima of transmitted radiation can be related not only to Fabry–Perot resonances but also to the maxima of $t_N^{(2)}$. Such maxima can be interpreted as excitation of Bloch surface plasmons on the rear boundary of the metal film. At the same time, coefficients $t_N^{(1)}$ have no maxima even in the case of finite-diameter holes. Because of this, excitation of Bloch surface plasmons on the front boundary of the metal film do not give rise to transmission coefficient maxima. Their influence can be manifested in the appearance of the reflection coefficient maxima.

6.2. The Case of Finite-Diameter Holes

We considered above the limiting case of a small-diameter hole ($k_0 d \to 0$). In the general case, coefficients r_{NM}, $t_N^{(2)}$ are found from the system of equations (24), (25). This system of equations is infinite and therefore its solution can be found only approximately. To find the solution, we pass on to the finite system of equations

$$h_{nm}^{(N)} + \sum_{M=0}^{M_{\max}} r_{NM} h_{nm}^{(M)} + h_{nm}^{\text{ref}} = h_{nm}^{t}, \tag{42}$$

$$\hat{\varepsilon}^{-1}\left(q_N h_{nm}^{(N)} - \sum_{M=0}^{M_{\max}} q_M r_{NM} h_{nm}^{(M)} - q h_{nm}^{\text{ref}}\right) = \frac{k_z}{\varepsilon_{1,2}} h_{nm}^t. \quad (43)$$

In Eqs. (42), (43), unlike (24), (25), summation over M is performed for a finite number of modes. The number $M_{\max}$ of considered modes determines the accuracy of solving the system of equations (24), (25). The contribution from all other modes is taken into account in the form of the term

$$h_{nm}^{\text{ref}} = \sum_{M=M_{\max}+1}^{\infty} r_{NM} h_{nm}^{(M)} \quad (44)$$

in Eq. (42) and the term $-qh_{nm}^{\text{ref}}$ in Eq. (43), where $q = k_0\sqrt{\varepsilon_M}$. Here, we took into account that the eigen-wavevector of the mode q_M tends to q with increasing the mode number. Therefore, we can reduce the infinite number of modes with numbers $M > M_{\max}$ to one effective mode with the wavevector q.

The system of equations (42), (43) allows us to find coefficients r_{NM}, $t_N^{(2)}$ with any preliminarily specified accuracy. However, it is difficult for analytic consideration. To find analytic expressions for positions of the maxima of coefficients r_{NM} and $t_N^{(2)}$, we will assume that

$$\sum_M r_{NM} h_{nm}^{(M)} \approx r_{NM'} h_{nm}^{(M')},$$

$$\sum_M q_M r_{NM} h_{nm}^{(M)} \approx q_{M'} r_{NM'} h_{nm}^{(M')}$$

at the maximum of r_{NM}. As a result, we obtain the system of equations

$$h_{nm}^{(N)} + r_{NM} h_{nm}^{(M)} = h_{nm}^t, \quad (45)$$

$$\hat{\varepsilon}^{-1}(q_N h_{nm}^{(N)} - q_M r_{NM} h_{nm}^{(M)}) = \frac{k_z}{\varepsilon_{1,2}} h_{nm}^t. \quad (46)$$

We are interested in the mode reflection coefficients $r_N^{(1)}$, $r_N^{(2)}$ of “the hole in metal–dielectric interface,” which coincide with coefficients r_{NN}. Therefore, we will consider only the case of $N = M$. In this case,

$$(1 + r_{NN}) h_{nm}^{(N)} = h_{nm}^t, \quad (47)$$

$$\hat{\varepsilon}^{-1} h_{nm}^{(N)} q_N (1 - r_{NN}) = \frac{k_z}{\varepsilon_{1,2}} h_{nm}^t. \quad (48)$$

By solving Eqs. (47), (48), we can no longer assume that the tensor $\hat{\varepsilon}^{-1} \approx \varepsilon_M^{-1}\hat{I}$, where $\hat{I}$ is the unit matrix. Indeed, in this case,

$$\varepsilon_{00}^{-1} = \left(1 - \frac{\pi d^2}{4L^2}\right)\varepsilon_M^{-1} + \frac{\pi d^2}{4L^2}\varepsilon_H^{-1} \quad (49)$$

and

$$\varepsilon_{nm}^{-1} \sim \frac{\pi d^2}{4L^2}\varepsilon_H^{-1}, \quad (50)$$

where ε_H is the permittivity in the hole. Therefore, it seems that, when $L^2 \gg d^2$, we can assume that $\varepsilon_{00}^{-1} \approx \varepsilon_M^{-1}$ and $\varepsilon_{nm}^{-1} \approx 0$. However, as a rule, $|\varepsilon_M| \gg \varepsilon_{1,2}$ and coefficients ε_{00}^{-1} and ε_{10}^{-1}, ε_{11}^{-1}, ... prove to be of the same order of magnitude. For example, in the case of a gold metal film perforated by a periodic array of holes with diameter d = 100–150 nm and period L = 400–600 nm,

$$\frac{\pi d^2}{4L^2} = 0.022\text{–}0.11, \quad (51)$$

and

$$|\varepsilon_M \varepsilon_H^{-1}| \approx 10. \quad (52)$$

Therefore, for $d \approx 150$ nm and $L \approx 400$ nm, we have $|\varepsilon_{00}^{-1}| \approx |\varepsilon_{10}^{-1}| \approx |\varepsilon_{11}^{-1}|$. Therefore, in Eqs. (47), (48), along with ε_{00}^{-1}, it is necessary to take into account coefficients ε_{10}^{-1}, ε_{11}^{-1}, ...[8]

For each pair of values of n and m, the effective permittivity can be introduced as

$$\varepsilon_{\text{eff}}(n,m) = \left(\frac{\sum_{i,j} \varepsilon_{ij}^{-1} h_{ij}^{(N)}}{h_{nm}^{(N)}}\right)^{-1}. \quad (53)$$

By using the effective permittivity, the reflection coefficient can be written in the form

$$r_{NN} = \frac{\varepsilon_{1,2} q_N - \varepsilon_{\text{eff}} k_z}{\varepsilon_{1,2} q_N + \varepsilon_{\text{eff}} k_z}. \quad (54)$$

The coefficient r_{NN} has a maximum under the resonance condition

$$\varepsilon_{1,2} q_N + \varepsilon_{\text{eff}} k_z = 0. \quad (55)$$

Condition (55) is fulfilled when the tangential component of the wavevector $\mathbf{k}_{nm}$ is

$$|\mathbf{k}_{nm}| = k_{\text{res}} = \sqrt{\varepsilon_{1,2}\frac{\omega^2}{c^2} - \frac{\varepsilon_{1,2}^2}{\varepsilon_{\text{eff}}^2} q_N^2}. \quad (56)$$

In other words, the maxima of the reflection coefficient r_{NN} are observed under the condition

$$k_{\text{res}} = \left|\frac{2\pi}{L_x} n\mathbf{e}_x + \frac{2\pi}{L_y} m\mathbf{e}_y\right|. \quad (57)$$

[8] When $d < 100$ nm and $L > 600$ nm, $|\varepsilon_{00}^{-1}| \gg |\varepsilon_{10}^{-1}|$ and we can assume approximately that $\hat{\varepsilon}^{-1} \approx \varepsilon_M^{-1}\hat{I}$, where $\hat{I}$ is the unit matrix.

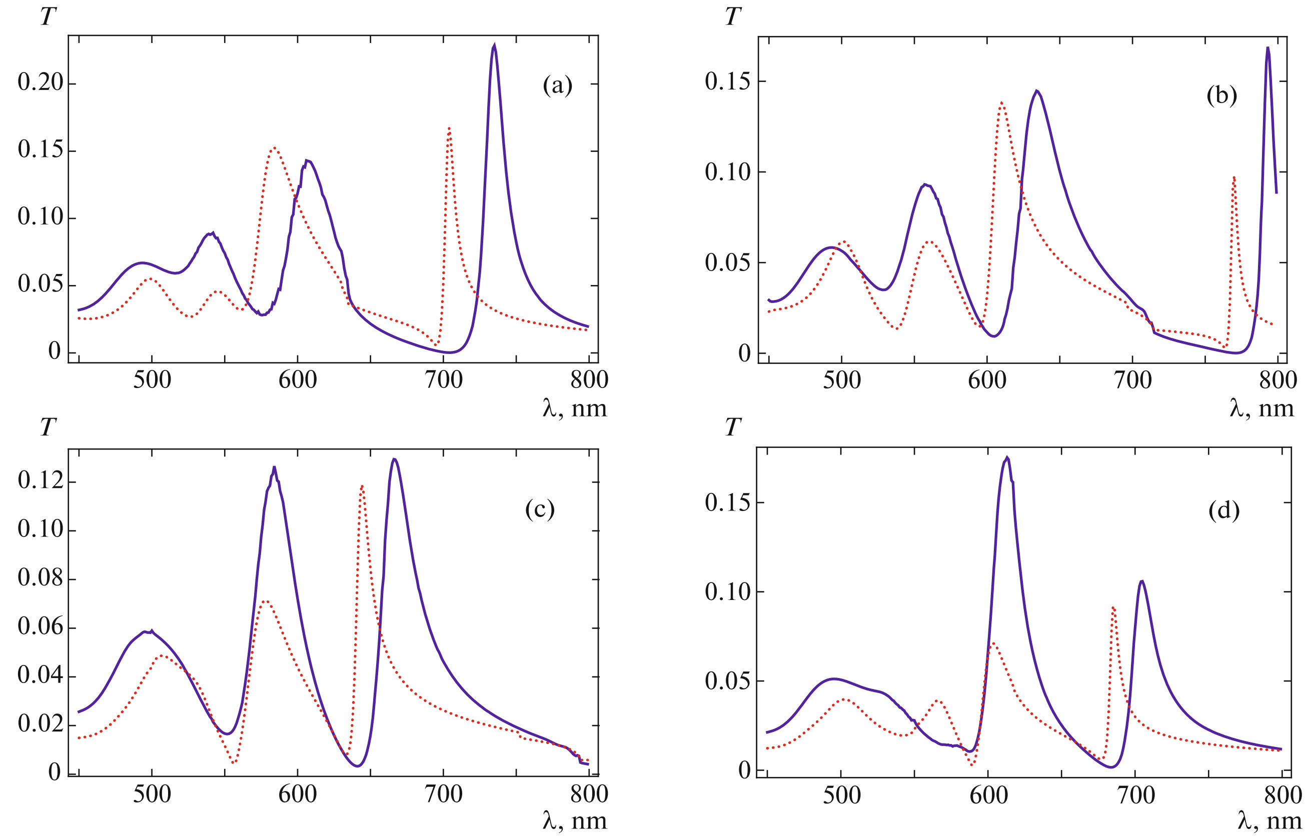

Fig. 6. Wavelength dependences of the transmission coefficient. Solid curves correspond to numerical calculations, dotted curves to analytic calculations. The film thickness is 100 nm, the hole diameter is 150 nm, the array period is W_L = 400 (a), 450 (b), 500 (c), and 550 nm (d).

It follows from Eq. (57) that the positions of maxima of the transmission coefficient $t_N^{(2)}$ coincide with those of the reflection coefficient r_{NN}. Unlike the case of an infinitesimal hole diameter, the positions of maxima of $t_N^{(2)}$ are independent of n and m and are determined by the position of the maximum of r_{NN}. In particular, the transmission coefficient maximum is observed for a wave with the zero tangential component of the wavevector. Such a wave propagates without decay with distance from the rear boundary of the metal film and transfers energy away from the film.

Thus, in the case of finite-thickness holes, the intensity maxima of transmitted radiation can be related both to excitation of Fabry–Perot resonances in holes and excitation of Bloch plasmon modes on the rear boundary of the metal film.

7. COMPARISON OF ANALYTIC RESULTS WITH NUMERICAL CALCULATIONS

7.1. Transmission Coefficient Spectrum

To test the theory constructed, we compare transmission coefficients of a metal film perforated by a hole array obtained from the system equations (47), (48) with the results of numerical simulation using the Comsol Multiphysics 5.2 software (Fig. 6).

One can see from Fig. 6 that the theory qualitatively correctly describes all the maxima of the transmission coefficient. Moreover, it well enough predicts the position and intensity of the maxima and minima of the transmission coefficient (Fig. 6). The discrepancy between analytic results and numerical calculations is explained by the single-mode approximation used in calculations (see Section 4.1).

7.2. Dependence of the Transmission Coefficient on the Film Thickness

We showed in the previous section that maxim of the transmission coefficient can be related to Fabry–Perot resonances in holes, Bloch plasmon modes on the rear boundary of the metal film and "transmission windows" of metals. The intensities of transmission maxima related to Fabry–Perot resonances and Bloch plasmon modes differently depend on the film thickness.

The maxima of the transmission coefficient related to Bloch plasmon modes are proportional to $\exp(-h\mathrm{Im}q_N)$, where q_N is the wavevector of the most slowly decaying eigenmode of the hole. In our case, this the TE_{11}

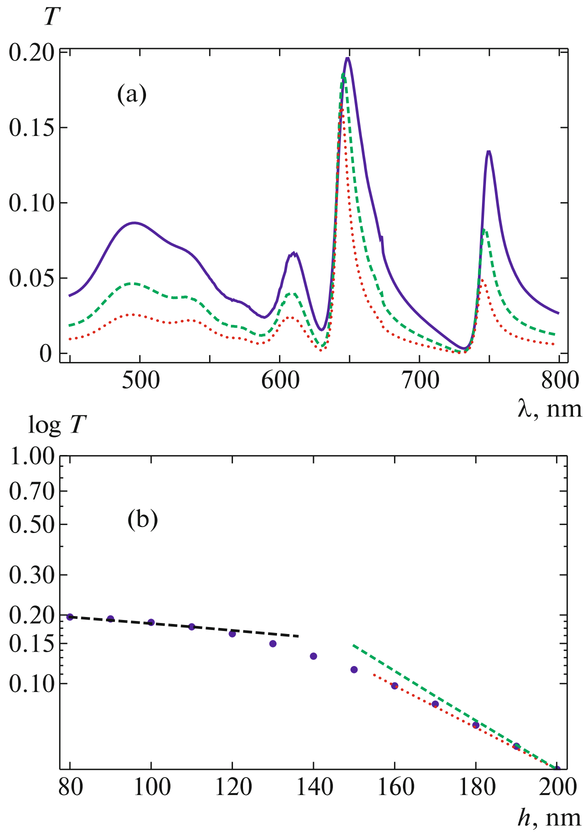

Fig. 7. (Color online) (a) Wavelength dependences of the transmission coefficient. The hole diameter is 150 nm, the array period is $L = 600$ nm, the film thickness is 80 nm (blue solid curve), 100 nm (green solid curve), and 120 nm (red dash-and-dot curve). (b) Dependences of the transmission coefficient on the film thickness at the maximum at about 650 nm. The hole diameter is 150 nm, the array period is $L = 600$ nm. The green curve is the decay decrement of the most slowly decaying eigenmode of the hole. The red and black curves show the real decay decrement for film thicknesses 100 and 180 nm.

mode. In turn, the maxima of the transmission coefficient related to Fabry–Perot resonances in holes are proportional to

$$\frac{\exp(-h\,\mathrm{Im}\,q_N)}{|1 - r_N^1 r_N^{(2)} \exp(2iq_N h)|} = \exp(-\gamma(h)h), \quad (58)$$

where $\gamma(h)$ is the decay decrement of the transmission coefficient. It follows from Eq. (58) that

$$\gamma(h) = \mathrm{Im}\,q_N + \frac{1}{h}\ln(|1 - r_N^1 r_N^{(2)} \exp(2iq_N h)|). \quad (59)$$

Near the Fabry–Perot resonance,

$$|1 - r_N^1 r_N^{(2)} \exp(2iq_N h)| \ll 1$$

and, as a result, $\gamma(h) < \mathrm{Im}q_N$.

Thus, transmission coefficient maxima related to Fabry–Perot resonance in holes decrease with increasing the film thickness slower than the amplitude of the most slowly decreasing eigenmode of the hole ($\gamma(h) < \mathrm{Im}q_N$).

Numerical simulations of the transmission coefficient of a gold film perforated by an array of holes confirm that the transmission coefficient maximum related to Fabry–Perot resonances in holes (for $\lambda \approx$ 650 nm) decreases much slower than all other maxima (Fig. 7a). Moreover, this maximum decreases with increasing the film thickness slower than the amplitude of the most slowly decreasing eigenmode q_N of the hole (Fig. 7b).

Different dependences of the amplitudes of transmission coefficient maxima related to Fabry–Perot resonances or Bloch plasmon modes on the rear boundary of the metal film on the film thickness allow us to simply determine the mechanism of the maximum appearance.

8. CONCLUSIONS

The appearance of transmission coefficient maxima is explained be three different mechanisms. Each mechanism dominates in a certain region of parameters.

First, transmission coefficient maxima appear in “the transparency window” of real metals (gold, silver, etc.), i.e., at frequencies where the absorption minimum is observed. The amplitude of the electromagnetic wave on the rear boundary of a metal film is equal to the sum of amplitudes of electromagnetic waves transmitted through holes in the metal film and the amplitudes of electromagnetic waves transmitted through the metal. When the amplitudes of waves transmitted through holes and metal are close, the transmission coefficient has two (or more) maxima at wavelengths close to the “transparency window” of the metal.

Second, transmission coefficient maxima can appear due to excitation of Fabry–Perot resonance in holes in the metal film described in [17].

Third, transmission coefficient maxima can appear due to excitation of Bloch surface plasmon modes on the rear boundary of the metal film.

It was shown in our paper that excitation of plasmon modes on the front boundary of the metal film does not produce transmission coefficient maxima.

It was also shown that in the “thick” film limit (the film thickness $h > 100$ nm), transmission coefficient maxima related to excitation of Fabry–Perot resonances in holes are observed at frequencies for which the excitation condition for surface resonances on the front and rear boundaries of the metal film is fulfilled.

We also showed that the amplitudes of the transmission coefficient maxima related to excitation of Fabry–Perot resonances in holes decrease with increasing the film thickness slower than the most slowly decaying mode of the hole.

ACKNOWLEDGMENTS

V.V. Klimov and A.A. Pavlov acknowledge the partial support of the Russian Foundation for Basic Research (project nos. 14-02-00290, 15-52-52006).

REFERENCES

1. T. W. Ebbesen, H. J. Lezec, H. F. Ghaemi, et al., Nature **391**, 667 (1998).
2. H. F. Ghaemi, T. Thio, D. E. Grupp, et al., Phys. Rev. B **58**, 6779 (1998).
3. F. J. Garcia de Abajo, Rev. Mod. Phys. **79**, 1267 (2007).
4. F. J. Garcia-Vidal, L. Martin-Moreno, T. W. Ebbesen, et al., Rev. Mod. Phys. **82**, 729 (2010).
5. H. J. Lezec, A. Degiron, E. Devaux, et al., Science **297**, 820 (2002).
6. H. A. Bethe, Phys. Rev. **66**, 163 (1944).
7. C. J. Bouwkamp, Philips. Res. Rep. **5**, 321 (1950).
8. C. J. Bouwkamp, Philips. Res. Rep. **5**, 401 (1950).
9. T. Thio, K. M. Pellerin, R. A. Linke, et al., Opt. Lett. **26**, 1972 (2001).
10. T. Thio, H. J. Lezec, T. W. Ebbesen, et al., Nanotechnology **13**, 429 (2002).
11. S.-H. Chang, S. K. Gray, and G. C. Schatz, Opt. Express **13**, 3150 (2005).
12. F. J. García-Vidal, E. Moreno, J. A. Porto, et al., Phys. Rev. Lett. **95**, 103901 (2005).
13. A. J. L. Adam, J. M. Brok, M. A. Seo, et al., Opt. Express **16**, 7407 (2008).
14. F. J. García-Vidal, L. Martín-Moreno, E. Moreno, et al., Phys. Rev. B **74**, 153411 (2006).
15. S. B. Cohn, Proc. IRE 40, 783 (1952).
16. J. A. Porto, F. J. García-Vidal, and J. B. Pendry, Phys. Rev. Lett. **83**, 2845 (1999).
17. L. Martín-Moreno, F. J. García-Vidal, H. J. Lezec, et al., Phys. Rev. Lett. **86**, 1114 (2001).
18. U. Schroter and D. Heitmann, Phys. Rev. B **58**, 419 (1998).
19. Z. Ruan and M. Qiu, Phys. Rev. Lett. **96**, 233901 (2006).
20. E. Popov, M. Neviere, S. Enoch, et al., Phys. Rev. B **62**, 16100 (2000).
21. Q. Cao and P. Lalanne, Phys. Rev. Lett. **88**, 057403 (2002).
22. A. D. Rakic, A. B. Djurisic, and J. M. Elazar, Appl. Opt. **37**, 5271 (1998).
23. O. Airy, *Essex Papers* (Camden Society, London, 1890).
24. C. A. Pfeiffer, E. N. Economou, and K. L. Ngai, Phys. Rev. B **10**, 3038 (1974).
25. J. A. Stratton, *Electromagnetic Theory* (McGraw-Hill, New York, 1941), p. 526.
26. L. A. Vainshtein, The Theory of Diffraction and the Factorization Method: Generalized Wiener-Hopf Technique, Golem Series in Electromagnetics (Sovetskoe Radio, Moscow, 1966; Golem, Boulder, CO, 1969), rus. p. 155.
27. L. D. Landau and E. M. Lifshitz, *Course of Theoretical Physics*, Vol. 8: *Electrodynamics of Continuous Media* (Fizmatlit, Moscow, 2005; Pergamon, New York, 1984), rus. p. 458.

Translated by M. Sapozhnikov